Surface Defines the Properties: Colloidal Bi2Se3 Nanosheets with High Electrical Conductivity

Christoph Bauer,[1,‡] Rostyslav Lesyuk,[2,3,‡] Mahdi Samadi Khoshkoo,[1] Christian Klinke,[2,4,*] Vladimir Lesnyak,[1,*] Alexander Eychmüller[1]

[1]*Physical Chemistry, TU Dresden, Zellescher Weg 19, 01069 Dresden, Germany*

[2]*Institute of Physics, University of Rostock, Albert-Einstein-Straße 23, 18059 Rostock, Germany*

[3]*Pidstryhach Institute for Applied Problems of Mechanics and Mathematics of NAS of Ukraine, Naukowa str. 3b, 79060 Lviv & Department of Photonics, Lviv Polytechnic National University, Bandery str. 12, 79000 Lviv, Ukraine*

[4]*Department of Chemistry, Swansea University – Singleton Park, Swansea SA2 8PP, UK*

[‡]these authors contributed equally to the work

Abstract: We investigated the colloidal synthesis of Bi_2Se_3 nanosheets in ethylene glycol with the goal of increasing their lateral dimensions while keeping their thickness within a few nanometers. The influence of proton-donating sulfuric acid was found to be a triggering factor that promoted the lateral growth of up to 10 µm, whereas the thickness remained in the range of 10–12 nm. The lateral size distribution was further optimized by size-selective precipitation enabling individual contacting of the nanosheets by electron-beam lithography. Electrical characterization of individually contacted nanosheets by e-beam lithography revealed metal-like temperature dependence of the resistivity and values of the specific conductivity in the range of 470 S/cm at room temperature and 880 S/cm at 5 K, which is attributed to the surface-induced off-stoichiometry. Presented colloidal nanosheets can potentially serve as a platform for further studies on topologically non-trivial surface states and arising quantum phenomena in two-dimensional systems.

Keywords: bismuth selenide nanosheets, colloidal synthesis, topological insulators, electron-beam lithography, specific conductivity.

INTRODUCTION

Bi_2Se_3 attracts growing attention of a broad researcher community as a layered semiconductor belonging to the class of so-called topological insulator prototypes. Initially it was studied as a thermoelectric material.[1,2] However, a large number of reports in the recent years carefully paved the way to deeply understanding the quantum-mechanical properties of this material and opened for it new areas such as spintronics. In fact, due to a strong spin-orbit coupling, the surface states of a topological insulator invert their orbital character to fulfill matching conditions at the interface with

vacuum or other materials with weak spin-orbit coupling. This leads to the formation of two crossing surface state bands which link bulk valence and conduction bands giving rise to the appearance of Dirac cones and metallic conduction. In contrast to regular surface states, spin-orbit coupling-induced surface bands are protected by topology and time-inversion symmetry, which makes them less sensitive to given surface conditions and orientation. Both theoretical and experimental studies (primarily, ARPES) showed the appearance of Dirac cones on the surface of topological insulators, in particular of Bi_2Se_3[3,4]. However, experimental evidences are rather scarce and refer to specific effects like the Aharonov-Bohm effect and Shubnikov-de-Haas oscillations[5]. Rarely, the electrical transport through Bi_2Se_3 nanostructures could be assigned to the contribution of topological surface states in Bi_2Se_3,[6] rather the opposite was frequently reported – their absence due to scattering for example[5]. It is to be expected that the contribution of surface states to the electrical transport increases with the reduction of the thickness of Bi_2Se_3 nanostructures. In this light, the colloidal synthesis route opens such a possibility being able to produce over-micrometer large nanosheets (NSs) with thicknesses down to 10 nm. Here, the surface presents a substantial part of the two-dimensional (2D) nanostructure being able to dominate the properties of a nanocrystal.

Wet-chemical synthesis procedures have been already shown to be a versatile tool to produce micrometer large NSs with nanoscale thicknesses. The increased surface-area of these NSs contributes strongly to the materials' properties, which can be utilized for surface-engineering.[7–9] Large Bi_2Se_3 NSs with lateral sizes far beyond 5 µm and thicknesses below 5 nm have been produced using chemical vapor deposition techniques.[10] However, the yield of chemical vapor deposition methods is very low in contrast to solvent-based procedures, and they require the use of designated substrates and expensive equipment.[10] In contrast to this, published wet-chemical routes so far yielded either sub-10 nm thin NSs with still rather insufficient lateral sizes of up to 2 µm,[11–13] or those reaching sizes of up to 10 µm, but having thicknesses above 10 nm.[14] In this work the focus is laid on the development of a facile wet-chemical procedure to obtain Bi_2Se_3 NSs with lateral sizes of up to 10 µm without increasing the thickness beyond 12 nm. Electrical properties of thus synthesized, individual NSs have been characterized after lithographic contacting. These measurements revealed rather high specific conductivity reaching 470 S/cm at room temperature and 880 S/cm upon cooling to 5.5 K and metal-like temperature dependence of the conductivity. We attribute this behavior to surface-induced off-stoichiometry found by X-ray photoelectron spectroscopy analysis. Nevertheless, the contribution of topologically protected surface states could not be excluded.

EXPERIMENTAL PART

Materials. Ethylene glycol (EG, ≥99.5%) and acetone (p.A.) were purchased from Honeywell Riedel-de Haen. Na_2SeO_3 (99%), $Bi(NO_3)_3{\cdot}5H_2O$ (99.999%), polyvinylpyrrolidone (PVP,

M_w=40kDa, 10 kDa, 360 kDa), and sulfuric acid (95-97%) were purchased from Sigma-Aldrich. Iso-propanol (iPrOH, p.A.) was purchased from Fisher.

Synthesis of Bi_2Se_3 NSs with large lateral dimensions.

The synthesis procedure was adapted from Lin et al.[11] with modifications in order to grow large Bi_2Se_3 NSs with lateral sizes above 5 µm and thickness of about 10 nm. For the synthesis of large Bi_2Se_3 NSs, 97 mg (0.2 mmol) of $Bi(NO_3)_3 \cdot 5H_2O$, 51.9 mg (0.3 mmol) of Na_2SeO_3, 666.9 mg (6 mmol) of polyvinylpyrrolidone (PVP) (Mw = 40 kDa), and 10 mL of ethylene glycol (EG) were mixed in a 25 mL three-neck flask with condenser attached. The solution was stirred for 1 h before adding 48 µL (0.9 mmol) of concentrated sulfuric acid and subsequent heating to 190°C. The reaction time at this temperature was set to 48 h. Thereafter, the mixture was cooled down to room temperature. The crude solution was centrifuged at 5000 rcf for 5 min (the scheme of the experiment is shown in Figure 1). The precipitate was kept, and the supernatant transferred into a second centrifuge tube. The centrifugation was repeated using the supernatant. This size-selective precipitation procedure was typically repeated 3 times. Then, the obtained precipitates were purified by adding iPrOH/acetone (1:1-vol.) mixture and centrifugation at 5000 rcf for 5 min. The supernatant was discarded, and the precipitate was redispersed in 5 mL of iPrOH with the help of an ultrasonic bath. 5 mL of acetone were added, and the suspension was centrifuged for 5 min. The last two steps were repeated three times. The obtained precipitate was redispersed in 5 mL iPrOH for further use.

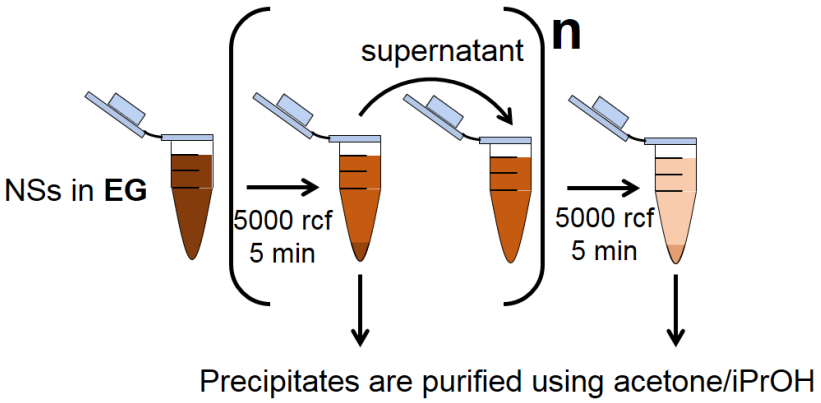

Figure 1. Size selective precipitation procedure used to remove too thick and too small NSs.

Characterization.

Morphology as well as elemental content were analyzed by ***scanning electron microscopy (SEM)*** on a SU8000 SE Microscope (Hitachi) operating at 1–2 kV, equipped with an ***energy dispersive X-ray spectroscopy (EDX)*** setup (from Oxford instruments) operating at 20 kV.

Samples for ***pH measurements*** were prepared by mixing 1 mL of the EG-based sample solution with 9 mL of deionized water. The analysis was then carried out using an inoLab pH 7110 device with attached glass electrode.

X-ray photoelectron spectroscopy (XPS) measurements were performed using a spectrometer equipped with a Scienta 200 analyzer and a monochromatized Al K_α X-ray source (1486.61 eV) at pressures below $5 \cdot 10^{-10}$ mbar. For high-resolution scans, the pass energy and the step size were set to 50 and 0.05 eV, respectively. For electrical charge correction, the C 1S sp^3 peak at the binding energy of 284.8 eV was utilized. Acquisition and storage of data were accomplished using SES software version 1.2.6. The data fitting was conducted using Gauss-Lorentz profiles.

X-ray diffraction (XRD) analysis of the NS samples was performed on a D2 Phaser (Bruker) using a Si wafer onto which the NS dispersions were drop-cast and subsequently dried. The diffraction pattern references were obtained from the ICDD database.

Atomic force microscopy (AFM) characterization. The height profiles of the NSs were measured by a JPK Nano Wizard 3 atomic force microscope in intermittent contact mode (air) on Si/SiOx substrates.

NSs-based device preparation and electrical measurements. Electron beam lithography was carried out on Si/SiO_2 substrates. A diluted colloidal solution of the Bi_2Se_3 NSs was spin-coated on the substrate and dried. The NSs were contacted individually by electron-beam lithography and thermal evaporation of 1/30 nm Ti/Au in two-point geometry with a gap size of 2–6 µm. As e-beam resist AR-P 632.06 PMMA (Allresist) was used. The produced devices were installed in a Lakeshore-Desert CRX closed-cycle probe station equipped with a Lakeshore 336 temperature controller for room and low temperature electrical measurements in vacuum (~10^{-5} mbar). The measurements were carried out with back-gate geometry, a highly doped silicon substrate with 300 nm thermal oxide as gate dielectric was used. For the illumination of the NSs, a red laser (λ = 630 nm) with up to 20 mW power was used. The electrical behavior was investigated and determined in a temperature range of 5–300 K using a Keithley 4200-SCS parameter analyzer.

RESULTS AND DISCUSSION

Synthesis and structural characterization of Bi_2Se_3 NSs

Large Bi_2Se_3 NSs with a thickness of about 10 nm and lateral dimensions of approximately 4.5 µm (up to 10 µm) were synthesized using an EG based method, with PVP as a stabilizer, according to the recipe of Lin et al.,[11] and with the addition of sulfuric acid. In our experiments we evaluated reaction time, temperature, amount of PVP, and pH as possible factors to increase the size of the NSs without increasing their thickness. From these experiments we found that changing the PVP concentration, temperature and reaction time alone did not lead to a significant increase of lateral dimensions of the Bi_2Se_3 NSs (see the Supporting Information for further details). To grow larger NSs an additional parameter needed to be varied, which we concluded to be the pH level of the reaction mixture. The formation of Bi_2Se_3 NSs is determined by the evolution of glycol aldehyde, which acts as a reducing

agent. In the course of the reaction, EG is oxidized to acetaldehyde at temperatures above 190°C (equation 1).[15,16]

$$HOCH_2CH_2OH \rightarrow CH_3CHO + H_2O \quad (1)$$

In our synthesis, sodium selenite is then reduced to a reactive selenium species by the formed acetaldehyde. In order to monitor the reaction, we sampled the product NSs at different times. For the samples taken after 30 min and 60 min the solution color changed from opaque white to red upon cooling, displaying that a component which has been dissolved at elevated temperatures precipitates upon cooling. The red precipitates were analyzed by XRD, which revealed that reactive selenide was formed in the early stages of the process. For the further insight, 1 mL of each sample was mixed with 10 mL of deionized water in order to evaluate the pH of these suspensions. The pH value shifted from acidic to basic over the course of the first two hours. We attribute this effect to the reaction of sodium selenite with the reducing agent acetaldehyde forming selenide (equation 2).

$$Na_2SeO_3 + 3\ CH_3CHO \rightarrow Na_2Se + 3\ CH_3COOH \uparrow \quad (2)$$

The side product of this reaction is acetic acid (boiling point at approximately 120°C), which evaporated out of the system at relatively high reaction temperatures, or is consumed by esterification and, therefore, does not affect the system's pH. The increase in pH could be explained by the strongly basic character of sodium selenide, which can react with a proton-donor such as EG to form sodium hydrogen selenide (equation 3):

$$Na_2Se + H_2O \rightarrow NaHSe + NaOH \quad (3)$$

Na_2Se as well as NaHSe are prone to oxidation and can decompose into polyselenides as well as elemental selenium.[11] During the reaction, the strong reducing conditions in EG will impede the oxidation to elemental selenium. However, taken samples are cooled down to room temperature, thereby acetaldehyde evolution stops, and the selenides can be oxidized rapidly. The reduction in pH after 90 min reaction can be attributed to the predominant reaction of the reactive selenide source with $Bi(NO_3)_3 \cdot 5H_2O$, forming Bi_2Se_3, given by the following equation:

$$3\ NaHSe + 2\ Bi(NO_3)_3 \cdot 5H_2O \rightarrow Bi_2Se_3 + 3\ NaNO_3 + 3\ HNO_3 \quad (4)$$

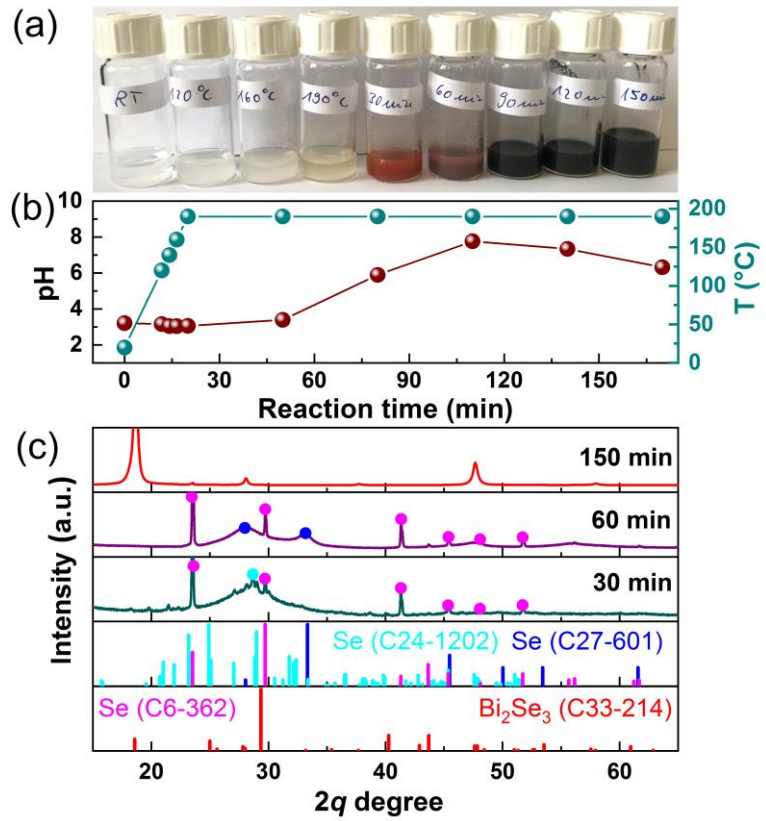

Figure 2. Photo of samples taken during the synthesis (a), changes of the pH value and reaction temperature over time (b), and XRD patterns of samples taken during the growth after 30, 60 and 150 min of reaction time (c).

This observation led to the assumption that changing the pH level may have a pronounce effect on the growth of the NSs. In order to confirm this, we investigated the impact of proton donating high-boiling sulfuric acid on the formation of Bi_2Se_3 NSs (for further details of the synthetic part see the SI). Indeed, employing this approach, we were able to synthesize large and thin sheets using 3 eq. of H_2SO_4 per Na_2SeO_3, increasing the amount of PVP by 3- to 5-fold and extending the reaction time up to 48–72 h (Figure 3). Size selective precipitation in EG was used to remove both, residues of thicker, as well as smaller nanocrystals. Using XRD analysis, the crystal structure of the product was determined to be rhombohedral. One drawback of our method is a relatively large distribution of sizes of the crystals, yet this distribution scales with the size of the produced NSs.

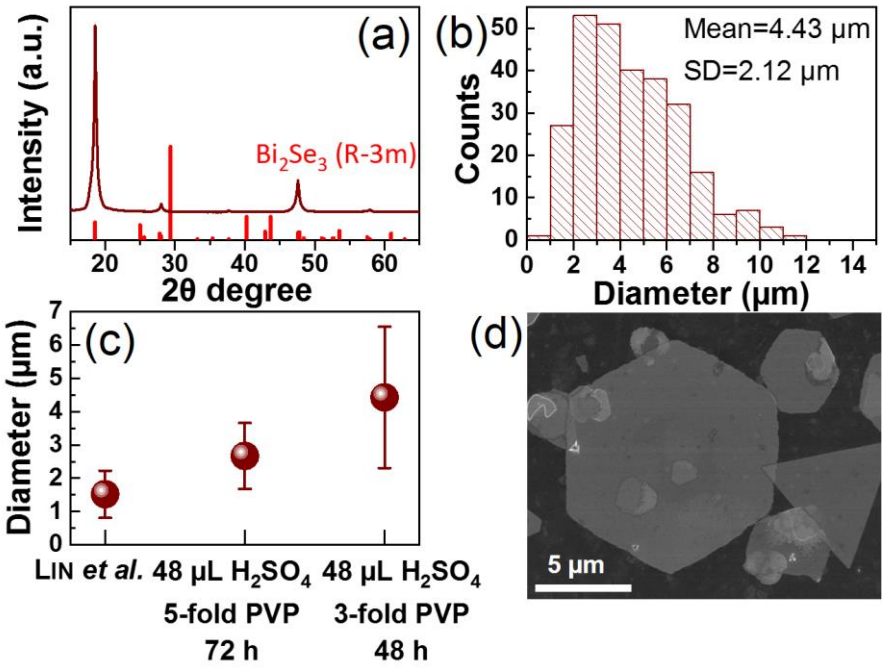

Figure 3. Comparison of XRD patterns (a) and size distribution (b) of our Bi_2Se_3 NSs obtained using the approach of Lin et al. and its modification. Variation of the NSs sizes depending on the reaction conditions (c) and SEM image (d) of large Bi_2Se_3 NSs.

Further, the performed XPS analysis gave insights into the chemical composition of the surface of the obtained NSs. As can be seen from Figure 4 in the Bi 4*f*-region, two components of bismuth exist in the samples. The main components at 157.7 and 163.1 eV, corresponding to Bi $4f_{7/2}$ and Bi $4f_{5/2}$, are related to Bi core atoms with a binding energy that corroborates well with the results reported in the literature for Bi_2Se_3[17]. The second components at 159.3 and 164.7 eV are attributed to oxidized Bi atoms on the surface of the NSs[18]. In the Se *3d*-region, we could only observe one component of selenium (a doublet centered at 53.3 and 54.2 eV, corresponded to Se $3d_{5/2}$ and Se $3d_{3/2}$), whose binding energy is in good accordance to the values reported in the literature for Bi_2Se_3. No other Se species (with different oxidation states/chemical surrounding) were detected, which suggests that the NSs are terminated with Bi atoms. In XPS as well as EDS analysis, no sulfur species were detected, indicating that sulfate ions from the sulfuric acid do not bind to the NS surface.

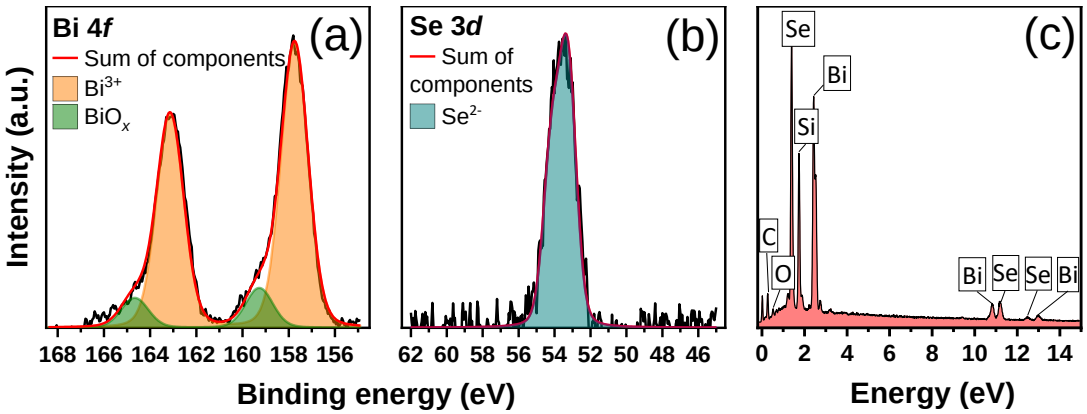

Figure 4. XPS scans and EDS profile of Bi_2Se_3 NSs: Bi 4*f* (a) and Se 3*d* (b) scans. The EDS profile of the large Bi_2Se_3 NSs (c).

Electrical transport properties of Bi_2Se_3 NSs

According to previous literature reports, Bi_2Se_3 films or pressed samples comprising of NSs or nanowires clearly showed a semiconductor behavior with increasing conductivity at temperature raise[19–21]. Researchers characterized the thermoelectric properties of these materials and found ways to improve them by doping/alloying with tellurium. They also reported Bi_2Se_3-nanoparticles based samples, which showed either an internal photo-effect being able to serve as ultra-sensitive photodetectors[22] or a thermoelectric effect[19]. It is worth to mention that the reported samples were fabricated from Bi_2Se_3 NSs with thicknesses of 10–20 nm (estimation from TEM)[22] and 50–100 nm[21]. In both cases, the authors noted the increased conductivity in comparison to earlier results and bulk Bi_2Se_3. Going down to thinner structures by exfoliation, Sun et al. showed a 2-fold improvement in conductivity in single-layer-based Bi_2Se_3 composites and explained this by a size effect on band structure, i.e. increased density of states near the conductance band and thus, improved mobility.[19] However, the temperature behavior in the 300–400 K range showed a semiconducting trend.

On the other hand, measurements on cleaved,[5,23,24] or molecular beam epitaxy-grown monocrystalline, physically prepared samples[4,25] as well as on Bi_2Se_3 nanostructures fabricated by the vapor-liquid-solid method[26] showed the opposite trend – pronounced metallic dependence of the conductivity versus temperature. This dependence was also observed by Lin et al. for the colloidal predecessor-nanoplates.[11] The reasons for the observed phenomenon are debated and are usually attributed to self-doping. Topologically protected surface states and nanosized surface effects are mentioned as well as other contributors.

To investigate the synthesized NSs in terms of electrical properties, we deposited them on Si/SiO_2 wafers and contacted them individually by e-beam lithography in two-point-contact geometry, as shown in Figure 5a, b. Optical microscopy and AFM were used to determine the position and thickness of each NS. We recorded I–V curves and probed the gating ability in field-effect transistor

measurements with gate voltage ranging from –10 to +10 V at different laser excitations and temperatures, as well as we determined electrical conductivities in a temperature range of 5–300 K using a vacuum probe-station and a parameter analyzer with a noise level of about 10^{-14} A. In Figure 5c the conductivity of a representative sample is shown as a function of temperature.

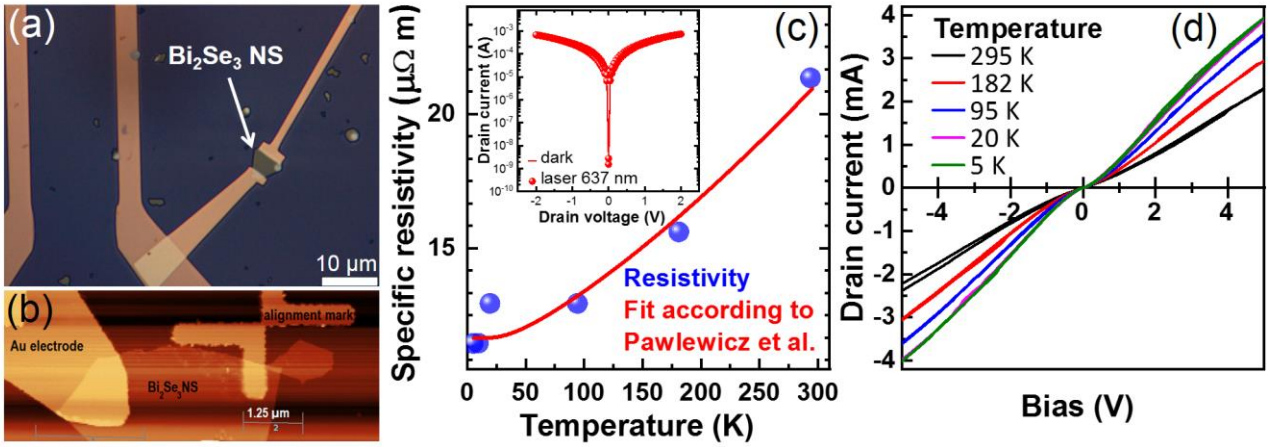

Figure 5. Optical microscope image of the substrate with gold contacts to Bi_2Se_3 NSs on a SiO_2/Si wafer (a). AFM image of the contact area: NS with electrode and alignment mark (b). Electrical characterization of single NSs (c): specific resistivity vs. temperature showing metallic behavior. Inset: I–V curves revealing no photoconductivity. I–V curves vs. temperature showing slight s-shaped dependence due to the residual contact resistance (c).

The measurements revealed a clear absence of a field effect in our samples as well as no photocurrent was observed (inset in Figure 5c). Instead, we found metallic behavior for the conductivity as a function of temperature and substantial values of conductivity in the range of $2.5 \cdot 10^4$ – $4.7 \cdot 10^4$ S/m at room temperature (Figure 5c, d). The experimental curve in Figure 5c (specific resistivity) comprises a shoulder in the range of 25 to 50 K. Possible reasons for the observed metallic behavior, in addition to self-doping effect, might include also the presence of metallic bismuth on the surface, carbonization of the surface or band structure peculiarities. Among the latter are conducting surface states, which can significantly contribute to the electrical transport making this pathway dominant in these thin NSs. Under given fabrication conditions, the carbonization of the whole surface of the NS can be excluded due to the presence of the PMMA resist during the evaporation of gold. Further, during fabrication and measurements the temperature in the chamber never exceeded 150 °C. The decomposition of PVP takes place only at temperatures above 300°C[27–29]. The appearance of massive metallic bismuth can be excluded by the XPS data. Despite the deviation of the stoichiometry from Bi:Se=2:3 in XPS, the excessive Bi cannot be ascribed to metallic bismuth (Bi-Bi), but according to the measured core-level shift should rather be attributed to the bismuth-terminated surface in the chemical environment of selenium and the ligands. Eventually, the electrical

conductivity of PVP should not have an effect on our measurements being more than tree orders of magnitude lower than the conductivity of Bi_2Se_3 and showing an opposite ρ vs. T trend[30]. Thus, the observed behavior can be completely linked to the intrinsic behavior of the Bi_2Se_3 NSs.

The red curve in Figure 5c represents the fit of the specific resistivity dependence on the temperature according to the phenomenological model of Pawlewicz et al. for doped Bi_2Se_3[31]. The Bloch-Grüneisen fit (typical for metals) with n=5 can also be applied and is presented in Figure SI9. To increase the quality of the fit, the Debye temperature was fixed to 182 K as has been found earlier for Bi_2Se_3[32]. We extracted the following parameters from the Pawlewicz-fit: residual resistance $R=1.2\cdot10^{-5}$ Ω, fitting parameters $\alpha=4.4\times10^{-5}$ $\Omega\cdot m\cdot K^{-2}$ and $\beta=10^{-10}$ Ω·m. From both fits, we may conclude the dominating role of electron-phonon scattering in the electrical transport and marginal contribution of electron-electron interaction. In the temperature range below 100 K, the measured values depart slightly from the fit indicating a more complex behavior at low temperatures, such as increased contribution of electron-electron scattering[4] or interaction with charged defects. Similar electrical transport signatures (ρ vs T) were observed by Butch et al.[5] in Bi_2Se_3 bulky single crystals with charge carrier concentrations of $n\sim10^{17}$ cm^{-1} and were linked to the corresponding Hall mobility behavior. The high scattering rates at the surface in their work were considered to be responsible for the inability to register the contribution of topologically non-trivial surface states to the electrical transport.

As mentioned above, a number of groups[4,5,11,23–25] already reported metallic behavior of Bi_2Se_3, which was referred to the self-doping as a consequence of Se vacancies present in the crystal structure. In our case this might be one of the valid reasons for our observations. In fact, in our XPS data we see the appearance of surface bismuth and no indications for selenium on the surface revealing the Bi-termination of lateral surfaces of NSs. The ratio of Bi:Se in this case for 10 nm thick NSs should deviate from the stoichiometric value of 0.67 to approx. 0.75. From the fitted XPS curves the Bi:Se ratio of 0.87 was calculated suggesting even larger deviation of the composition from the stoichiometric one towards selenium deficit in the atomic layers close to the surface (here we keep in mind the surface sensitivity of XPS). These findings could be an explanation for the observed metallic behavior. Surface-induced off-stoichiometry was already reported as a theoretical possibility for occurring mid-gap (surface) states at the Fermi level of PbS and the disappearance of the band gap at raising off-stoichiometry[33,34]. However, an effective passivation with surface cations reopens the band-gap[35] returning the sample its semiconducting properties. The surface bismuth in our case is linked to the PVP ligands and obviously to oxygen (Bi–O bond from XPS) and the possible dangling bonds producing metallic states are thus (at least partially) saturated. Hence, the contribution of topologically protected surface states to the observed transport behavior cannot be completely

excluded so far. ~~Hall and magnetoresistance measurements are needed to further study the metallic nature of the samples.~~

The band structure of bulk Bi_2Se_3 despite the semi-metallic character of Bi assumes the presence of a narrow direct band gap according to recent studies[36]. DFT simulations of a thin slab of Bi_2Se_3 reveal the appearance of a Dirac cone at the Γ point[3]. Further decrease of the thickness from approx. 5 to 1 nm causes the interaction between the states on opposite surfaces[37] leading to the reopening of the bandgap[38,39]. Our NSs comprise of nearly 10 quintuple layers and thus offering a highly suitable solution-processable platform for the study of charge carriers in topologically non-trivial surface states.

CONCLUSIONS

Over one micron large and yet thin Bi_2Se_3 NSs were synthesized using a colloidal approach. We determined the influence of proton donating sulfuric acid on the Bi_2Se_3 formation in an EG-mediated synthesis that promotes the lateral growth of NSs. Individual NSs reached up to 10 µm in lateral dimensions. The initial pronounced broad size distribution of NSs was reduced by size-selective precipitation. The thickness of these NSs varied typically in a range between 10 and 12 nm. According to our results, a further synthesis optimization reduces the wide size distribution, while maintaining the large lateral crystal sizes and thin 2D morphologies. Furthermore, we studied the electrical output and transfer characteristics of single NSs contacted by means of electron beam lithography. Individually contacted NSs showed high electrical conductivity with specific conductivities at room temperature reaching 470 S/cm and 880 S/cm at 5.5 K and a metal-like temperature dependence attributed to the surface-induced off-stoichiometry. However, the contribution of topologically protected surface states could not be excluded. the presented NSs with the achieved geometrical dimensions provide a suitable and convenient platform for further studies of spin-orbit coupling-based phenomena on the surface of topological insulators.

Supporting Information: Additional SEM images of the Bi_2Se_3 NSs, analysis of their size distribution, FTIR spectra, and the Bloch-Grüneisen function. This material is available free of charge *via* the Internet at http://pubs.acs.org.

Acknowledgments:

This work was supported by the German Research Foundation (DFG) within the International Excellence Graduate School on Emerging Materials and Processes Korea (iEGSEMP Korea) in the context of TU Dresden's Institutional Strategy "The Synergetic University". We thank Dr. A. Koitzsch (IFW-Dresden) for providing assistance in XPS measurements.

Corresponding Authors:

*E-mails: christian.klinke@uni-rostock.de, vladimir.lesnyak1@tu-dresden.de

Author Contributions:

The manuscript was written through the contributions of all authors. All authors have approved the final version of the manuscript.

References

(1) John, K. J.; Pradeep, B.; Mathai, E. Electrical properties of bismuth selenide (Bi_2Se_3) thin films prepared by reactive evaporation. Solid State Commun. 1993, 85, 879–881.

(2) Mishra, S. K.; Satpathy, S.; Jepsen, O. Electronic structure and thermoelectric properties of bismuth telluride and bismuth selenide. J. Phys.: Condens. Matter 1997, 9, 461.

(3) Xia, Y.; Qian, D.; Hsieh, D.; Wray, L.; Pal, A.; Lin, H.; Bansil, A.; Grauer, D.; Hor, Y. S.; Cava, R. J. Observation of a large-gap topological-insulator class with a single Dirac cone on the surface. Nat. Phys. 2009, 5, 398–402.

(4) Wang, J.; DaSilva, A. M.; Chang, C.-Z.; He, K.; Jain, J. K.; Samarth, N.; Ma, X.-C.; Xue, Q.-K.; Chan, M. H. W. Evidence for electron-electron interaction in topological insulator thin films. Phys. Rev. B 2011, 83, 245438.

(5) Butch, N. P.; Kirshenbaum, K.; Syers, P.; Sushkov, A. B.; Jenkins, G. S.; Drew, H. D.; Paglione, J. Strong surface scattering in ultrahigh-mobility Bi_2Se_3 topological insulator crystals. Phys. Rev. B 2010, 81, 241301.

(6) Veyrat, L.; Iacovella, F.; Dufouleur, J.; Nowka, C.; Funke, H.; Yang, M.; Escoffier, W.; Goiran, M.; Eichler, B.; Schmidt, O. G. Band bending inversion in Bi_2Se_3 nanostructures. Nano Lett. 2015, 15, 7503–7507.

(7) He, L.; Xiu, F.; Yu, X.; Teague, M.; Jiang, W.; Fan, Y.; Kou, X.; Lang, M.; Wang, Y.; Huang, G. Surface-dominated conduction in a 6 nm thick Bi_2Se_3 thin film. Nano Lett. 2012, 12, 1486–1490.

(8) Steinberg, H.; Gardner, D. R.; Lee, Y. S.; Jarillo-Herrero, P. Surface state transport and ambipolar electric field effect in Bi_2Se_3 nanodevices. Nano Lett. 2010, 10, 5032–5036.

(9) Yan, B.; Zhang, D.; Felser, C. Topological surface states of Bi_2Se_3 coexisting with Se vacancies. pps (RRL) 2013, 7, 148–150.

(10) Wang, F.; Li, L.; Huang, W.; Li, L.; Jin, B.; Li, H.; Zhai, T. Submillimeter 2D Bi_2Se_3 Flakes toward High‐Performance Infrared Photodetection at Optical Communication Wavelength. Adv. Funct. Mater. 2018, 28, 1802707.

(11) Lin, Z.; Chen, Y.; Yin, A.; He, Q.; Huang, X.; Xu, Y.; Liu, Y.; Zhong, X.; Huang, Y.; Duan, X. Solution processable colloidal nanoplates as building blocks for high-performance electronic thin films on flexible substrates. Nano Lett. 2014, 14, 6547–6553.

(12) Min, Y.; Moon, G. D.; Kim, B. S.; Lim, B.; Kim, J.-S.; Kang, C. Y.; Jeong, U. Quick, controlled synthesis of ultrathin Bi_2Se_3 nanodiscs and nanosheets. J. Am. Chem. Soc. 2012, 134, 2872–2875.

(13) Wu, X.; Tan, C.; Wang, Q.; Guo, Y.; Wang, D.; Wang, Y.; Meng, D. Solution growth of two-dimensional Bi_2Se_3 nanosheets for two-color all-optical switching. Materials 2017, 10, 1332.

(14) Zhou, F.; Zhao, Y.; Zhou, W.; Tang, D. Temperature-Dependent Raman Scattering of Large Size Hexagonal Bi_2Se_3 Single-Crystal Nanoplates. Appl. Sci. 2018, 8, 1794.

(15) Rodrigues, T. S.; Zhao, M.; Yang, T. ‐ H.; Gilroy, K. D.; da Silva, A. G. M.; Camargo, P. H. C.; Xia, Y. Synthesis of colloidal metal nanocrystals: A comprehensive review on the reductants. Chem. Eur. J. 2018, 24, 16944‐16963.

(16) Skrabalak, S. E.; Wiley, B. J.; Kim, M.; Formo, E. V.; Xia, Y. On the polyol synthesis of silver nanostructures: glycolaldehyde as a reducing agent. Nano Lett. 2008, 8, 2077–2081.

(17) Debies, T. P.; Rabalais, J. W. X-ray photoelectron spectra and electronic structure of Bi_2X_3 (X= O, S, Se, Te). Chem. Phys. 1977, 20, 277–283.

(18) Morgan, W. E.; Stec, W. J.; van Wazer, J. R. Inner-orbital binding-energy shifts of antimony and bismuth compounds. Inorg. Chem. 1973, 12, 953–955.

(19) Sun, Y.; Cheng, H.; Gao, S.; Liu, Q.; Sun, Z.; Xiao, C.; Wu, C.; Wei, S.; Xie, Y. Atomically thick bismuth selenide freestanding single layers achieving enhanced thermoelectric energy harvesting. J. Am. Chem. Soc. 2012, 134, 20294–20297.

(20) Xu, H.; Chen, G.; Jin, R.; Chen, D.; Pei, J.; Wang, Y. Electrical transport properties of microwave-synthesized $Bi_2Se_{3-x}Te_x$ nanosheet. CrystEngComm 2013, 15, 5626–5632.

(21) Xu, H.; Chen, G.; Jin, R.; Chen, D.; Wang, Y.; Pei, J.; Zhang, Y.; Yan, C.; Qiu, Z. Microwave-assisted synthesis of Bi_2Se_3 ultrathin nanosheets and its electrical conductivities. CrystEngComm 2014, 16, 3965–3970.

(22) Sharma, A.; Bhattacharyya, B.; Srivastava, A. K.; Senguttuvan, T. D.; Husale, S. High performance broadband photodetector using fabricated nanowires of bismuth selenide. Sci. Rep. 2016, 6, 19138.

(23) Checkelsky, J. G.; Hor, Y. S.; Liu, M.-H.; Qu, D.-X.; Cava, R. J.; Ong, N. P. Quantum interference in macroscopic crystals of nonmetallic Bi_2Se_3. Phys. Rev. Lett. 2009, 103, 246601.

(24) Cao, H.; Xu, S.; Miotkowski, I.; Tian, J.; Pandey, D.; Hasan, M. Z.; Chen, Y. P. Structural and electronic properties of highly doped topological insulator Bi_2Se_3 crystals. pss (RRL) 2013, 7, 133–135.

(25) Liu, M.; Chang, C.-Z.; Zhang, Z.; Zhang, Y.; Ruan, W.; He, K.; Wang, L.-l.; Chen, X.; Jia, J.-F.; Zhang, S.-C. Electron interaction-driven insulating ground state in Bi_2Se_3 topological insulators in the two-dimensional limit. Phys. Rev. B 2011, 83, 165440.

(26) Cha, J. J.; Williams, J. R.; Kong, D.; Meister, S.; Peng, H.; Bestwick, A. J.; Gallagher, P.; Goldhaber-Gordon, D.; Cui, Y. Magnetic doping and Kondo effect in Bi_2Se_3 nanoribbons. Nano Lett. 2010, 10, 1076–1081.

(27) Zhu, K.; Wang, G.; Zhang, S.; Du, Y.; Lu, Y.; Na, R.; Mu, Y.; Zhang, Y. Preparation of organic–inorganic hybrid membranes with superior antifouling property by incorporating polymer-modified multiwall carbon nanotubes. RSC Adv. 2017, 7, 30564–30572.

(28) Salles, T. H. C.; Lombello, C. B.; d'Ávila, M. A. Electrospinning of gelatin/poly(vinyl pyrrolidone) blends from water/acetic acid solutions. Mater. Res. 2015, 18, 509–518.

(29) Bauer, C.; Veremchuk, I.; Kunze, C.; Benad, A.; Dzhagan, V. M.; Haubold, D.; Pohl, D.; Schierning, G.; Nielsch, K.; Lesnyak, V. Heterostructured Bismuth Telluride Selenide Nanosheets for Enhanced Thermoelectric Performance. Small Sci., 2000021.

(30) Ravi, M.; Bhavani, S.; Pavani, Y.; Rao, V. V.R. Investigation on electrical and dielectric properties of PVP: KCLO 4 polymer electrolyte films. 0975-1041 2013.

(31) Pawlewicz, W. T.; Rayne, J. A.; Ure Jr, R. W. Resistivity of Bi_2Te_3 from 1.3 K to 300 K. Phys. Lett. A 1974, 48, 391–392.

(32) Shoemake, G. E.; Rayne, J. A.; Ure Jr, R. W. Specific heat of n-and p-type Bi_2Te_3 from 1.4 to 90 K. Phys. Rev. 1969, 185, 1046.

(33) Kim, D.; Kim, D.-H.; Lee, J.-H.; Grossman, J. C. Impact of stoichiometry on the electronic structure of PbS quantum dots. Phys. Rev. Lett. 2013, 110, 196802.

(34) Ramin Moayed, M. M.; Kull, S.; Rieckmann, A.; Beck, P.; Wagstaffe, M.; Noei, H.; Kornowski, A.; Hungria, A. B.; Lesyuk, R.; Stierle, A.; Klinke, C. Function Follows Form: From Semiconducting to Metallic toward Superconducting PbS Nanowires by Faceting the Crystal. Adv. Funct. Mater. 2020, 30, 1910503.

(35) Zherebetskyy, D.; Scheele, M.; Zhang, Y.; Bronstein, N.; Thompson, C.; Britt, D.; Salmeron, M.; Alivisatos, P.; Wang, L.-W. Hydroxylation of the surface of PbS nanocrystals passivated with oleic acid. Science 2014, 344, 1380–1384.

(36) Martinez, G.; Piot, B. A.; Hakl, M.; Potemski, M.; Hor, Y. S.; Materna, A.; Strzelecka, S. G.; Hruban, A.; Caha, O.; Novák, J. Determination of the energy band gap of Bi_2Se_3. Sci. Rep. 2017, 7, 1–5.

(37) Brahlek, M.; Koirala, N.; Bansal, N.; Oh, S. Transport properties of topological insulators: Band bending, bulk metal-to-insulator transition, and weak anti-localization. Solid State Commun. 2015, 215, 54–62.

(38) Yazyev, O. V.; Moore, J. E.; Louie, S. G. Spin polarization and transport of surface states in the topological insulators Bi_2Se_3 and Bi_2Te_3 from first principles. Phys. Rev. Lett. 2010, 105, 266806.
(39) Sapkota, Y. R.; Mazumdar, D. Bulk transport properties of bismuth selenide thin films grown by magnetron sputtering approaching the two-dimensional limit. J. Appl. Phys. 2018, 124, 105306.